Inorg. Chem. **2005**, *44*, 6100–6110

Synthesis, Characterization, Crystal Structure, and Electrochemical, Photophysical, and Protein-Binding Properties of Luminescent Rhenium(I) Diimine Indole Complexes

Kenneth Kam-Wing Lo,*,† Keith Hing-Kit Tsang,† Wai-Ki Hui,† and Nianyong Zhu‡

Department of Biology and Chemistry, City University of Hong Kong, Tat Chee Avenue, Kowloon, Hong Kong, P. R. China, and Department of Chemistry, The University of Hong Kong, Pokfulam Road, Hong Kong, P. R. China

Received April 7, 2005

We report the synthesis, characterization, and photophysical and electrochemical properties of a series of luminescent rhenium(I) diimine indole complexes, $[Re(N–N)(CO)_3(L)](CF_3SO_3)$ (N–N = 3,4,7,8-tetramethyl-1,10-phenanthroline (Me_4-phen), L = *N*-(3-pyridoyl)tryptamine (py-3-$CONHC_2H_4$-indole) (**1a**), *N*-[*N*-(3-pyridoyl)-6-aminohexanoyl]tryptamine, (py-3-$CONHC_5H_{10}CONHC_2H_4$-indole) (**1b**); N–N = 1,10-phenanthroline (phen), L = py-3-$CONHC_2H_4$-indole (**2a**), py-3-$CONHC_5H_{10}CONHC_2H_4$-indole (**2b**); N–N = 2,9-dimethyl-1,10-phenanthroline (Me_2-phen), L = py-3-$CONHC_2H_4$-indole (**3a**), py-3-$CONHC_5H_{10}CONHC_2H_4$-indole (**3b**); N–N = 4,7-diphenyl-1,10-phenanthroline (Ph_2-phen), L = py-3-$CONHC_2H_4$-indole (**4a**), py-3-$CONHC_5H_{10}CONHC_2H_4$-indole (**4b**)), and their indole-free counterparts, $[Re(N–N)(CO)_3(py\text{-}3\text{-}CONH\text{-}Et)](CF_3SO_3)$ (py-3-CONH-Et = *N*-ethyl-(3-pyridyl)formamide; N–N = Me_4-phen (**1c**), phen (**2c**), Me_2-phen (**3c**), Ph_2-phen (**4c**)). The X-ray crystal structure of complex **3a** has also been investigated. Upon irradiation, most of the complexes exhibited triplet metal-to-ligand charge-transfer (^{3}MLCT) ($d\pi(Re) \rightarrow \pi^*$(diimine)) emission in fluid solutions at 298 K and in low-temperature glass. However, the structural features and long emission lifetimes of the Me_4-phen complexes in solutions at room temperature suggest that the excited state of these complexes exhibited substantial triplet intraligand (^{3}IL) ($\pi \rightarrow \pi^*$) (Me_4-phen) character. The binding interactions of these complexes to indole-binding proteins including bovine serum albumin and tryptophanase have been examined.

Introduction

The indole unit occurs naturally in a variety of structures, and over a thousand indole alkaloids are known to date. Due to the wide existence and the important physiological activities of these indole compounds,[1] the search for their specific receptors has been met with increasing attention. The design of biological probes for indole-binding proteins relies mainly on functionalized indole derivatives. In fact, the fluorescence of indole and its derivatives is sensitive to the environment and, thus, these compounds have been exploited as reporters of their surroundings.[2,3] Various indole derivatives, such as those connected to organic fluorophores or radioactive species, have been employed in the identification and isolation of indole-binding proteins.[3,4] In view of the remarkable luminescence properties of rhenium(I) diimine complexes,[5−17] we have recently utilized two luminescent rhenium(I) diimine indole complexes $[Re(Me_4\text{-phen})(CO)_3(L)](CF_3SO_3)$ (Me_4-phen = 3,4,7,8-tetramethyl-1,10-phenanthroline; L = *N*-(3-pyridoyl)tryptamine, (py-3-$CONHC_2H_4$-indole) (**1a**), *N*-[*N*-(3-pyridoyl)-6-aminohexanoyl]tryptamine, (py-3-$CONHC_5H_{10}CONHC_2H_4$-indole) (**1b**)) as probes for

* Author to whom all correspondence should be addressed. E-mail: bhkenlo@cityu.edu.hk. Fax: (852) 2788 7406. Tel: (852) 2788 7231.
† City University of Hong Kong.
‡ The University of Hong Kong.

(1) See, for example: Ishida, T.; Hamada, M.; Inoue, M.; Wakahara, A. *Chem. Pharm. Bull.* **1990**, *38*, 851−855. Bartel, B. *Annu. Rev. Plant Physiol.* **1997**, *48*, 51−66.
(2) Schore, N. E.; Turro, N. J. *J. Am. Chem. Soc.* **1975**, *97*, 2488−2496.
(3) Mazzini, A.; Cavatorta, P.; Iori, M.; Favilla, R.; Sartor, G. *Biophys. Chem.* **1992**, *42*, 101−109.
(4) Zettl, R.; Schell, J.; Palme, K. *Proc. Natl. Acad. Sci. U.S.A.* **1994**, *91*, 689−693.
(5) Wrighton, M. S.; Morse, D. L. *J. Am. Chem. Soc.* **1974**, *96*, 998−1003. Giordano, P. J.; Wrighton, M. S. *J. Am. Chem. Soc.* **1979**, *101*, 2888−2897.
(6) (a) Wallace, L.; Jackman, D. C.; Rillema, D. P.; Merkert, J. W. *Inorg. Chem.* **1995**, *34*, 5210−5214. (b) Villegas, J. M.; Stoyanov, S. R.; Huang, W.; Rillema, D. P. *Dalton Trans.* **2005**, 1042−1051.

10.1021/ic050531u CCC: $30.25
Published on Web 07/22/2005

Chart 1

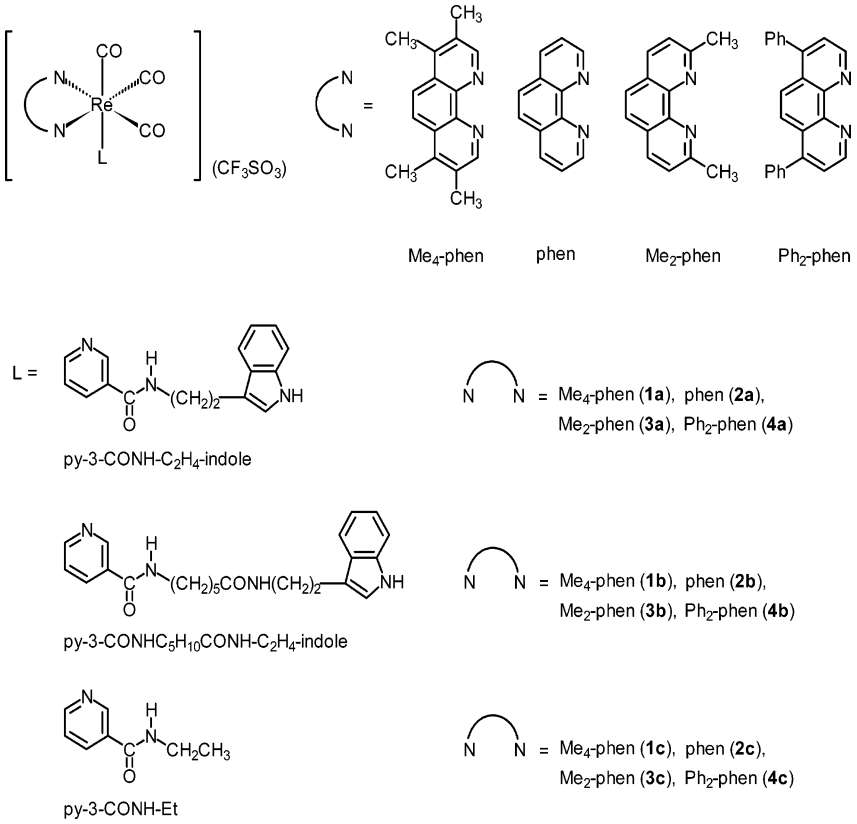

indole-binding proteins including bovine serum albumin (BSA) and tryptophanase (TPase).[17c] Whereas the indole moiety can serve as the biological recognition unit for these proteins, the luminescent rhenium(I) diimine units provide environment-sensitive emission that could assist in the detection, monitoring, and isolation of these important biomolecules. In this paper, we report the synthesis and characterization of a new series of luminescent rhenium(I) diimine indole complexes, $[Re(N-N)(CO)_3(L)](CF_3SO_3)$ (N−N = 1,10-phenanthroline (phen), L = py-3-$CONHC_2H_4$-indole (**2a**), py-3-$CONHC_5H_{10}CONHC_2H_4$-indole (**2b**); N−N = 2,9-dimethyl-1,10-phenanthroline (Me_2-phen), L = py-3-$CONHC_2H_4$-indole (**3a**), py-3-$CONHC_5H_{10}CONHC_2H_4$-indole (**3b**); N−N = 4,7-diphenyl-1,10-phenanthroline (Ph_2-phen), L = py-3-$CONHC_2H_4$-indole (**4a**), py-3-$CONHC_5H_{10}CONHC_2H_4$-indole (**4b**)), and their indole-free counterparts, $[Re(N-N)(CO)_3(py\text{-}3\text{-}CONH\text{-}Et)](CF_3SO_3)$ (py-3-CONH-Et = *N*-ethyl-(3-pyridyl)formamide; N−N = phen (**2c**), Me_2-phen (**3c**), Ph_2-phen (**4c**)) (Chart 1). The photophysical and electrochemical properties of these new complexes have been studied. The binding of these complexes to BSA and the inhibition of TPase by these complexes have also been examined.

(7) (a) Westmoreland, T. D.; Le Bozec, H.; Murray, R. W.; Meyer, T. J. *J. Am. Chem. Soc.* **1983**, *105*, 5952−5954. (b) Chen, P.; Duesing, R.; Graff, D. K.; Meyer, T. J. *J. Phys. Chem.* **1991**, *95*, 5850−5858. (c) Mecklenburg, S. L.; Opperman, K. A.; Chen, P.; Meyer, T. J. *J. Phys. Chem.* **1996**, *100*, 15145−15151. (d) López, R.; Leiva, A. M.; Zuloaga, F.; Loeb, B.; Norambuena, E.; Omberg, K. M.; Schoonover, J. R.; Striplin, D.; Devenney, M.; Meyer, T. J. *Inorg. Chem.* **1999**, *38*, 2924−2930. (e) Claude, J. P.; Omberg, K. M.; Williams, D. S.; Meyer, T. J. *J. Phys. Chem. A* **2002**, *106*, 7795−7806.

(8) (a) Stoeffler, H. D.; Thornton, N. B.; Temkin, S. L.; Schanze, K. S. *J. Am. Chem. Soc.* **1995**, *117*, 7119−7128. (b) Thornton, N. B.; Schanze, K. S. *New J. Chem.* **1996**, *20*, 791−800. (c) Lucia, L. A.; Abboud, K.; Schanze, K. S. *Inorg. Chem.* **1997**, *36*, 6224−6234.

(9) (a) Lees, A. J. *Chem. Rev.* **1987**, *87*, 711−743. (b) Sun, S.-S.; Lees, A. J.; Zavalij, P. Y. *Inorg. Chem.* **2003**, *42*, 3445−3453.

(10) (a) Juris, A.; Campagna, S.; Bidd, I.; Lehn, J,-M.; Ziessel, R. *Inorg. Chem.* **1988**, *27*, 4007−4011. (b) Ziessel, R.; Juris, A.; Venturi, M. *Chem. Commun.* **1997**, 1593−1594.

(11) (a) Moya, S. A.; Guerrero, J.; Pastene, R.; Schmidt, R.; Sariego, R.; Sartori, R.; Sanz-Aparicio, J.; Fonseca, I.; Martínez-Ripoll, M. *Inorg. Chem.* **1994**, *33*, 2341−2346. (b) Guerrero, J.; Piro, O. E.; Wolcan, E.; Feliz, M. R.; Ferraudi, G.; Moya, S. A. *Organometallics* **2001**, *20*, 2842−2853.

(12) (a) Sacksteder, L.; Zipp, A. P.; Brown, E. A.; Streich, J.; Demas, J. N.; DeGraff, B. A. *Inorg. Chem.* **1990**, *29*, 4335−4340. (b) Zipp, A. P.; Sacksteder, L.; Streich, J.; Cook, A.; Demas, J. N.; DeGraff, B. A. *Inorg. Chem.* **1993**, *32*, 5629−5632.

(13) (a) Hino, J. K.; Ciana, L. D.; Dressick, W. J.; Sullivan, B. P. *Inorg. Chem.* **1992**, *31*, 1072−1080. (b) Schutte, E.; Helms, J. B.; Woessner, S. M.; Bowen, J.; Sullivan, B. P. *Inorg. Chem.* **1998**, *37*, 2618−2619.

(14) (a) Yoblinski, B. J.; Stathis, M.; Guarr, T. F. *Inorg. Chem.* **1992**, *31*, 5−10. (b) Lin, R.; Fu, Y.; Brock, C. P.; Guarr, T. F. *Inorg. Chem.* **1992**, *31*, 4346−4353.

(15) Rossenaar, B. D.; Stufkens, D. J.; Vlček, A., Jr. *Inorg. Chim. Acta* **1996**, *247*, 247−255.

(16) Yam, V. W. W.; Lo, K. K. W.; Cheung, K. K.; Kong, R. Y. C. *J. Chem. Soc., Chem. Commun.* **1995**, 1191−1993. Yam, V. W. W.; Lo, K. K. W.; Cheung, K. K.; Kong, R. Y. C. *J. Chem. Soc., Dalton Trans.* **1997**, 2067−2072.

(17) (a) Lo, K. K. W.; Hui, W. K.; Ng, D. C. M.; Cheung, K. K. *Inorg. Chem.* **2002**, *41*, 40−46. (b) Lo, K. K. W.; Hui, W. K.; Ng, D. C. M. *J. Am. Chem. Soc.* **2002**, *124*, 9344−9345. (c) Lo, K. K. W.; Tsang, K. H. K.; Hui, W. K.; Zhu, N. *Chem. Commun.* **2003**, 2704−2705. (d) Lo, K. K. W.; Lau, J. S. Y.; Fong, V. W. Y.; Zhu, N. *Organometallics* **2004**, *23*, 1098−1106. (e) Lo, K. K. W.; Hui, W. K. *Inorg. Chem.* **2005**, *44*, 1992−2002.

Experimental Section

Materials and General Methods. All solvents were of analytical reagent grade. Chloropentacarbonylrhenium(I) (Aldrich), tryptamine (Aldrich), nicotinoyl chloride hydrochloride (Aldrich), diimine ligands (N−N) (Aldrich), *N*-hydroxysuccinimide (Acros), BSA (Calbiochem), lactate dehydrogenase from porcine heart (Calbiochem), β-nicotinamide adenine dinucleotide, disodium salt (NADH) (Calbiochem), TPase (Sigma), and pyridoxal 5-phosphate (Sigma) were used without purification. Nicotinic acid *N*-hydroxysuccinimidyl ester, py-3-CONHC$_2$H$_4$-indole, py-3-CONHC$_5$H$_{10}$-CONHC$_2$H$_4$-indole, py-3-CONH-Et, and complexes **1a**−**c** were prepared as described previously.[17c]

[Re(phen)(CO)$_3$(py-3-CONHC$_2$H$_4$-indole)](CF$_3$SO$_3$) (2a). A mixture of [Re(phen)(CO)$_3$(CH$_3$CN)](CF$_3$SO$_3$) (160 mg, 0.25 mmol) and py-3-CONHC$_2$H$_4$-indole (66 mg, 0.25 mmol) in 20 mL of anhydrous THF was refluxed under nitrogen for 12 h. The solution was evaporated to dryness to give an orange-yellow solid. Subsequent recrystallization from acetonitrile/acetone/diethyl ether afforded complex **2a** as yellow crystals. Yield: 186 mg (86%). ^{1}H NMR (300 MHz, acetone-d_6, 298 K, relative to TMS): δ 10.07 (s, 1H, NH of indole ring), 9.93 (dd, 2H, J = 5.3 and 1.5 Hz, H2 and H9 of phen), 9.09 (dd, 2H, J = 8.5 and 1.2 Hz, H4 and H7 of phen), 8.86 (d, 1H, J = 2.1 Hz, H2 of pyridine), 8.73 (d, 1H, J = 5.0 Hz, H6 of pyridine), 8.37−8.33 (m, 4H, H3, H5, H6 and H8 of phen), 8.27−8.24 (m, 1H, H4 of pyridine), 8.10 (s, 1H, py-3-CON*H*), 7.63 (d, 1H, J = 7.9 Hz, H4 of indole ring), 7.46−7.39 (m, 2H, H5 of pyridine and H7 of indole ring), 7.15−7.08 (m, 2H, H2 and H6 of indole ring), 7.00 (t, 1H, J = 7.5 Hz, H5 of indole ring), 3.63−3.56 (m, 2H, NHC*H*$_2$CH$_2$), 2.95 (t, 2H, J = 7.3 Hz, NHCH$_2$C*H*$_2$). Anal. Calcd for [Re(phen)(CO)$_3$(py-3-CONHC$_2$H$_4$-indole)](CF$_3$SO$_3$)·H$_2$O·0.25(CH$_3$)$_2$CO: C, 43.83; H, 2.98; N, 7.80. Found: C, 43.69; H, 2.76; N, 7.55. IR (KBr; ν/cm^{-1}): 3432 (m, NH), 2034 (s, C≡O), 1916 (s, C≡O), 1650 (m, C═O), 1158 (m, $CF_3SO_3^-$), 1030 (m, $CF_3SO_3^-$). Positive-ion ESI-MS ion clusters (*m*/*z*): 715, {[Re(phen)(CO)$_3$(py-3-CONHC$_2$H$_4$-indole)]}$^+$; 450, {[Re(phen)(CO)$_3$]}$^+$.

[Re(phen)(CO)$_3$(py-3-CONHC$_5$H$_{10}$CONHC$_2$H$_4$-indole)](CF$_3$SO$_3$) (2b). The preparation of complex **2b** was similar to that of complex **2a** except that py-3-CONHC$_5$H$_{10}$CONHC$_2$H$_4$-indole (95 mg, 0.25 mmol) was used instead of py-3-CONHC$_2$H$_4$-indole. Complex **2b** was isolated as yellow crystals. Yield: 156 mg (64%). ^{1}H NMR (300 MHz, acetone-d_6, 298 K, relative to TMS): δ 10.00 (s, 1H, NH of indole ring), 9.91 (d, 2H, J = 5.3 Hz, H2 and H9 of phen), 9.06 (d, 2H, J = 8.5 H, H4 and H7 of phen), 8.81 (s, 1H, H2 of pyridine), 8.72 (d, 1H, J = 6.2 Hz, H6 of pyridine), 8.36−8.27 (m, 4H, H3, H5, H6 and H8 of phen), 8.28 (d, 1H, J = 7.9 Hz, H4 of pyridine), 8.00 (s, 1H, py-3-CON*H*), 7.53 (d, 1H, J = 7.6 Hz, H4 of indole ring), 7.41−7.34 (m, 2H, H7 of indole ring and H5 of pyridine), 7.11−6.93 (m, 4H, CON*H*-C$_2$H$_4$-indole and H2, H5 and H6 of indole ring), 3.49−3.36 (m, 4H, py-3-CONHC*H*$_2$C$_4$H$_8$CONHC*H*$_2$CH$_2$), 2.13 (t, 2H, J = 7.0 Hz, py-3-CONHC$_4$H$_8$C*H*$_2$), 1.62−1.24 (m, 6H, py-3-CONHCH$_2$C$_3$*H*$_6$CH$_2$). Anal. Calcd for [Re(phen)(CO)$_3$(py-3-CONHC$_5$H$_{10}$CONHC$_2$H$_4$-indole)](CF$_3$SO$_3$): C, 46.67; H, 3.50; N, 8.59. Found: C, 46.55; H, 3.72; N, 8.40. IR (KBr; ν/cm^{-1}): 3370 (m, NH), 2033 (s, C≡O), 1919 (s, C≡O), 1655 (m, C═O), 1153 (m, $CF_3SO_3^-$), 1024 (m, $CF_3SO_3^-$). Positive-ion ESI-MS ion clusters (*m*/*z*): 829 {[Re(phen)(CO)$_3$(py-3-CONHC$_5$H$_{10}$CONHC$_2$H$_4$-indole)]}$^+$; 451, {[Re(phen)(CO)$_3$]}$^+$.

[Re(phen)(CO)$_3$(py-3-CONH-Et)](CF$_3$SO$_3$) (2c). The preparation of complex **2c** was similar to that of complex **2a** except that py-3-CONH-Et (38 mg, 0.25 mmol) was used instead of py-3-CONHC$_2$H$_4$-indole. Complex **2c** was isolated as yellow crystals. Yield: 81 mg (43%). ^{1}H NMR (300 MHz, acetone-d_6, 298 K, relative to TMS): δ 9.94 (d, 2H, J = 5.0 Hz, H2 and H9 of phen), 9.91 (d, 2H, J = 8.5 Hz, H4 and H7 of phen), 8.85 (s, 1H, H2 of pyridine), 8.56 (d, 1H, J = 5.9 Hz, H6 of pyridine), 8.39−8.35 (m, 4H, H3, H5, H6 and H8 of phen), 8.30−8.26 (m, 1H, H4 of pyridine), 8.03 (s, 1H, py-3-CON*H*), 7.44 (dd, 1H, J = 7.8 and 5.7 Hz, H5 of pyridine), 3.33−3.24 (m, 2H, py-3-CONHC*H*$_2$CH$_3$), 1.07 (t, 3H, J = 7.3 Hz, py-3-CONHCH$_2$C*H*$_3$). Anal. Calcd for [Re(phen)(CO)$_3$(py-3-CONH-Et)](CF$_3$SO$_3$)·0.5H$_2$O: C, 37.99; H, 2.52; N, 7.38. Found: C, 38.05; H, 2.60; N, 7.53. IR (KBr; ν/cm^{-1}): 3431 (m, NH), 2034 (s, C≡O), 1923 (s, C≡O), 1655 (m, C═O), 1152 (m, $CF_3SO_3^-$), 1030 (m, $CF_3SO_3^-$). Positive-ion ESI-MS ion clusters (*m*/*z*): 601, {[Re(phen)(CO)$_3$(py-3-CONH-Et)]}$^+$; 451, {[Re(phen)(CO)$_3$]}$^+$.

[Re(Me$_2$-phen)(CO)$_3$(py-3-CONHC$_2$H$_4$-indole)](CF$_3$SO$_3$) (3a). The preparation of complex **3a** was similar to that of complex **2a** except that [Re(Me$_2$-phen)(CO)$_3$(CH$_3$CN)](CF$_3$SO$_3$) (167 mg, 0.25 mmol) was used instead of [Re(phen)(CO)$_3$(CH$_3$CN)](CF$_3$SO$_3$). Complex **3a** was isolated as pale yellow crystals. Yield: 163 mg (73%). ^{1}H NMR (300 MHz, acetone-d_6, 298 K, relative to TMS): δ 10.08 (s, 1H, NH of indole ring), 8.81 (d, 2H, J = 8.5 Hz, H4 and H7 of Me$_2$-phen), 8.34 (d, 1H, J = 2.1 Hz, H2 of pyridine), 8.27 (d, 1H, J = 5.6 Hz, H6 of pyridine), 8.24 (d, 2H, J = 8.2 Hz, H3 and H8 of Me$_2$-phen), 8.20 (d, 1H, J = 8.2 Hz, H4 of pyridine), 8.12 (s, 2H, H5 and H6 of Me$_2$-phen), 8.06 (s, 1H, py-3-CON*H*), 7.55 (d, 1H, J = 7.9 Hz, H4 of indole ring), 7.40 (d, 1H, J = 7.3 Hz, H7 of indole ring), 7.31 (dd, 1H, J = 7.9 and 5.6 Hz, H5 of pyridine), 7.14−7.08 (m, 2H, H2 and H6 of indole ring), 6.99 (t, 1H, J = 7.0 Hz, H5 of indole ring), 3.70−3.54 (m, 2H, NHC*H*$_2$CH$_2$), 3.49 (s, 6H, Me at C2 and C9 of Me$_2$-phen), 2.95 (t, 2H, J = 7.0 Hz, NHCH$_2$C*H*$_2$). Anal. Calcd for [Re(Me$_2$-phen)(CO)$_3$(py-3-CONHC$_2$H$_4$-indole)](CF$_3$SO$_3$)·1.5H$_2$O: C, 44.39; H, 3.29; N, 7.61. Found: C, 44.41; H, 3.55; N, 7.84. IR (KBr; ν/cm^{-1}): 3339 (m, NH), 2034 (s, C≡O), 1910 (s, C≡O), 1660 (m, C═O), 1153 (m, $CF_3SO_3^-$), 1030 (m, $CF_3SO_3^-$). Positive-ion ESI-MS ion clusters (*m*/*z*): 744, {[Re(Me$_2$-phen)(CO)$_3$(py-3-CONHC$_2$H$_4$-indole)]}$^+$; 477, {[Re(Me$_2$-phen)(CO)$_3$]}$^+$.

[Re(Me$_2$-phen)(CO)$_3$(py-3-CONHC$_5$H$_{10}$CONHC$_2$H$_4$-indole)](CF$_3$SO$_3$) (3b). The preparation of complex **3b** was similar to that of complex **2b** except that [Re(Me$_2$-phen)(CO)$_3$(CH$_3$CN)](CF$_3$SO$_3$) (167 mg, 0.25 mmol) was used instead of [Re(phen)(CO)$_3$(CH$_3$CN)](CF$_3$SO$_3$). Yield: 126 mg (50%). Complex **3b** was isolated as yellow crystals. ^{1}H NMR (300 MHz, acetone-d_6, 298 K, relative to TMS): δ 10.03 (s, 1H, NH of indole ring), 8.83 (d, 2H, J = 8.5 Hz, H4 and H7 of Me$_2$-phen), 8.32−8.25 (m, 5H, H3 and H8 of Me$_2$-phen and H2, H4 and H6 of pyridine), 8.11 (s, 2H, H5 and H6 of Me$_2$-phen), 7.96 (s, 1H, py-3-CON*H*), 7.56 (d, 1H, J = 7.6 Hz, H4 of indole ring), 7.37 (d, 1H, J = 8.2 Hz, H7 of indole ring), 7.29 (dd, 1H, J = 7.9 and 5.6 Hz, H5 of pyridine), 7.15−6.95 (m, 4H, CON*H*C$_2$H$_4$-indole and H2, H5, and H6 of indole ring), 3.49 (s, 6H, Me at C2 and C9 of Me$_2$-phen), 3.47−3.36 (m, 4H, py-3-CONHC*H*$_2$C$_4$H$_8$CONHC*H*$_2$CH$_2$), 2.89 (t, 2H, J = 7.3 Hz, NHCH$_2$C*H*$_2$-indole), 2.15 (t, 2H, J = 7.0 Hz, py-3-CONHC$_4$H$_8$C*H*$_2$), 1.60−1.25 (m, 6H, py-3-CONHCH$_2$C$_3$*H*$_6$CH$_2$). Anal. Calcd for [Re(Me$_2$-phen)(CO)$_3$(py-3-CONHC$_5$H$_{10}$CONHC$_2$H$_4$-indole)](CF$_3$SO$_3$)·2H$_2$O·CH$_3$CN: C, 46.57; H, 4.19; N, 9.05. Found: C, 46.35; H, 4.17; N, 9.27. IR (KBr; ν/cm^{-1}): 3400 (m, NH), 2032 (s, C≡O), 1919 (s, C≡O), 1650 (m, C═O), 1153 (m, $CF_3SO_3^-$), 1030 (m, $CF_3SO_3^-$). Positive-ion ESI-MS ion clusters (*m*/*z*): 857, {[Re(Me$_2$-phen)(CO)$_3$(py-3-CONHC$_5$H$_{10}$CONHC$_2$H$_4$-indole)]}$^+$; 479, {[Re(Me$_2$-phen)(CO)$_3$]}$^+$.

[Re(Me$_2$-phen)(CO)$_3$(py-3-CONH-Et)](CF$_3$SO$_3$) (3c). The preparation of complex **3c** was similar to that of complex **2c** except that [Re(Me$_2$-phen)(CO)$_3$(CH$_3$CN)](CF$_3$SO$_3$) (167 mg, 0.25 mmol) was used instead of [Re(phen)(CO)$_3$(CH$_3$CN)](CF$_3$SO$_3$). Complex **3c** was isolated as yellow crystals. Yield: 47 mg (24%). ^{1}H NMR (300 MHz, acetone-d_6, 298 K, relative to TMS): δ 8.85 (d, 2H, J = 9.4 Hz, H4 and H7 of Me$_2$-phen), 8.37 (s, 1H, H2 of pyridine), 8.35−8.27 (m, 3H, H3 and H8 of Me$_2$-phen and H6 of pyridine), 8.22 (d, 1H, J = 7.9 Hz, H4 of pyridine), 8.15 (s, 2H, H5 and H6 of Me$_2$-phen), 7.93 (s, 1H, py-3-CON*H*), 7.33 (dd, 1H, J = 8.5 and 5.8 Hz, H5 of pyridine), 3.50 (s, 6H, Me at C2 and C9 of Me$_2$-phen), 3.41−3.16 (m, 2H, py-3-CONHC*H*$_2$CH$_3$), 1.08 (t, 3H, J = 7.3 Hz, py-3-CONHCH$_2$C*H*$_3$). Anal. Calcd for [Re(Me$_2$-phen)(CO)$_3$(py-3-CONH-Et)](CF$_3$SO$_3$)·H$_2$O·0.5CH$_3$CN: C, 39.73; H, 3.15; N, 7.72. Found: C, 39.59; H, 2.98; N, 7.62. IR (KBr; ν/cm^{-1}): 3447 (m, NH), 2028 (s, C≡O), 1931 (s, C≡O), 1644 (m, C═O), 1153 (m, $CF_3SO_3^-$), 1025 (m, $CF_3SO_3^-$). Positive-ion ESI-MS ion clusters (*m*/*z*): 629, {[Re(Me$_2$-phen)(CO)$_3$(py-3-CONH-Et)]}$^+$; 477, {[Re(Me$_2$-phen)(CO)$_3$]}$^+$.

[Re(Ph$_2$-phen)(CO)$_3$(py-3-CONHC$_2$H$_4$-indole)](CF$_3$SO$_3$) (4a). The preparation of complex **4a** was similar to that of complex **2a** except that [Re(Ph$_2$-phen)(CO)$_3$(CH$_3$CN)]CF$_3$SO$_3$ (160 mg, 0.25 mmol) was used instead of [Re(phen)(CO)$_3$(CH$_3$CN)](CF$_3$SO$_3$). Complex **4a** was isolated as orange-yellow crystals. Yield: 200 mg (79%). ^{1}H NMR (300 MHz, acetone-d_6, 298 K, relative to TMS): δ 10.06 (s, 1H, NH of indole ring), 9.98 (d, 2H, J = 5.3 Hz, H2 and H9 of Ph$_2$-phen), 8.95 (s, 1H, H2 of pyridine), 8.81 (d, 1H, J = 5.3 Hz, H6 of pyridine), 8.30−8.28 (m, 3H, H3 and H8 of Ph$_2$-phen and H4 of pyridine), 8.23 (s, 2H, H5 and H6 of Ph$_2$-phen), 8.13 (s, 1H, py-3-CON*H*), 7.72−7.67 (m, 10H, Ph of Ph$_2$-phen), 7.55 (d, 1H, J = 7.6 Hz, H4 of indole ring), 7.48 (t, 1H, J = 7.0 Hz, H5 of pyridine), 7.38 (d, 1H, J = 7.9 Hz, H7 of indole ring), 7.16 (s, 1H, H2 of indole ring), 7.09 (t, 1H, J = 7.5 Hz, H6 of indole ring), 6.97 (t, 1H, J = 7.5 Hz, H5 of indole ring), 3.63−3.56 (m, 2H, NHC*H*$_2$CH$_2$), 2.96 (t, 2H, J = 7.2 Hz, NHCH$_2$C*H*$_2$). Anal. Calcd for [Re(Ph$_2$-phen)(CO)$_3$(py-3-CONHC$_2$H$_4$-indole)](CF$_3$SO$_3$)·H$_2$O·0.25CH$_3$CN: C, 49.13; H, 3.06; N, 6.61. Found: C, 48.84; H, 3.26; N, 6.86. IR (KBr; ν/cm^{-1}): 3148 (m, NH), 2031 (s, C≡O), 1918 (s, C≡O), 1654 (m, C═O), 1165 (m, $CF_3SO_3^-$), 1029 (m, $CF_3SO_3^-$). Positive-ion ESI-MS ion clusters (*m*/*z*): 867, {[Re(Ph$_2$-phen)(CO)$_3$(py-3-CONHC$_2$H$_4$-indole)]}$^+$; 602, {[Re(Ph$_2$-phen)(CO)$_3$]}$^+$.

[Re(Ph$_2$-phen)(CO)$_3$(py-3-CONHC$_5$H$_{10}$CONHC$_2$H$_4$-indole)](CF$_3$SO$_3$) (4b). The preparation of complex **4b** was similar to that of complex **2b** except that [Re(Ph$_2$-phen)(CO)$_3$(CH$_3$CN)](CF$_3$SO$_3$) (195 mg, 0.25 mmol) was used instead of [Re(phen)(CO)$_3$(CH$_3$CN)](CF$_3$SO$_3$). Yield: 150 mg (60%). Complex **4b** was isolated as yellow crystals. ^{1}H NMR (300 MHz, acetone-d_6, 298 K, relative to TMS): δ 10.06 (s, 1H, NH of indole ring), 9.98 (d, 2H, J = 5.3 Hz, H2 and H9 of Ph$_2$-phen), 8.94 (s, 1H, H2 of pyridine), 8.81 (d, 2H, J = 5.6 Hz, H6 of pyridine), 8.34 (d, 1H, H4 of pyridine), 8.28 (d, 2H, H3 and H8 of Ph$_2$-phen), 8.20 (s, 2H, H5 and H6 of Ph$_2$-phen), 8.14 (s, 1H, py-3-CON*H*), 7.68 (s, 10H, Ph of Ph$_2$-phen), 7.56 (d, 1H, J = 7.9 Hz, H4 of indole ring), 7.44 (dd, 1H, J = 7.6 and 5.8 Hz, H5 of pyridine), 7.34 (d, 1H, J = 8.2 Hz, H7 of indole ring), 7.16−6.91 (m, 4H, CON*H*C$_2$H$_4$-indole and H2, H5, and H6 of indole ring), 3.46−3.23 (m, 4H, py-3-CONHC*H*$_2$C$_4$H$_8$CONHC*H*$_2$CH$_2$), 2.86 (t, 2H, J = 7.3 Hz, NHCH$_2$C*H*$_2$-indole), 2.10 (t, 2H, J = 7.3 Hz, py-3-CONHC$_4$H$_8$C*H*$_2$), 1.58−1.23 (m, 6H, py-3-CONHCH$_2$C$_3$*H*$_6$CH$_2$). Anal. Calcd for [Re(Ph$_2$-phen)(CO)$_3$(py-3-CONHC$_5$H$_{10}$CONHC$_2$H$_4$-indole)](CF$_3$SO$_3$)·H$_2$O·CH$_3$CN: C, 52.52; H, 3.98; N, 8.24. Found: C, 52.31; H, 4.09; N, 8.25. IR (KBr; ν/cm^{-1}): 3132 (m, NH), 2023 (s, C≡O), 1910 (s, C≡O), 1645 (m, C═O), 1157 (m, $CF_3SO_3^-$), 1025 (m, $CF_3SO_3^-$). Positive-ion ESI-MS ion clusters (*m*/*z*): 857, {[Re(Ph$_2$-phen)(CO)$_3$(py-3-CONHC$_5$H$_{10}$CONHC$_2$H$_4$-indole)]}$^+$; 479, {[Re(Ph$_2$-phen)(CO)$_3$]}$^+$.

[Re(Ph$_2$-phen)(CO)$_3$(py-3-CONH-Et)](CF$_3$SO$_3$) (4c). The preparation of complex **4c** was similar to that of complex **2c** except that [Re(Ph$_2$-phen)(CO)$_3$(CH$_3$CN)]CF$_3$SO$_3$ (160 mg, 0.25 mmol) was used instead of [Re(phen)(CO)$_3$(CH$_3$CN)](CF$_3$SO$_3$). Complex **4c** was isolated as yellow crystals. Yield: 104 mg (46%). ^{1}H NMR (300 MHz, acetone-d_6, 298 K, relative to TMS): δ 10.00 (d, 2H, J = 5.3 Hz, H2 and H9 of Ph$_2$-phen), 8.95 (s, 1H, H2 of pyridine), 8.81 (d, 1H, J = 5.6 Hz, H6 of pyridine), 8.33−8.31 (m, 3H, H3 and H8 of Ph$_2$-phen and H4 of pyridine), 8.24 (s, 2H, H5 and H6 of Ph$_2$-phen), 8.01 (s, 1H, py-CON*H*), 7.73−7.68 (m, 10H, Ph of Ph$_2$-phen), 7.49 (dd, 1H, J = 7.9 and 5.6 Hz, H5 of pyridine), 3.36−3.25 (m, 2H, py-CONHC*H*$_2$CH$_3$), 1.08 (t, 3H, J = 7.3 Hz, py-CONHCH$_2$C*H*$_3$). Anal. Calcd for [Re(Ph$_2$-phen)(CO)$_3$(py-3-CONH-Et)](CF$_3$SO$_3$)·H$_2$O: C, 47.00; H, 3.07; N, 6.09. Found: C, 46.90; H, 3.16; N, 6.02. IR (KBr; ν/cm^{-1}): 3349 (m, NH), 2032 (s, C≡O), 1920 (s, C≡O), 1664 (m, C═O), 1155 (m, $CF_3SO_3^-$), 1029 (m, $CF_3SO_3^-$). Positive-ion ESI-MS ion clusters (*m*/*z*): 753, {[Re(Ph$_2$-phen)(CO)$_3$(py-3-CONH-Et)]}$^+$; 603, {[Re(Ph$_2$-phen)(CO)$_3$]}$^+$.

X-ray Structural Analysis for Complex 3a. Single crystals of the complex suitable for X-ray crystallographic studies were obtained by slow diffusion of diethyl ether vapor into a mixture of acetonitrile/acetone solution of the complex. A crystal of dimensions 0.4 × 0.2 × 0.1 mm^3 mounted in a glass capillary was used for data collection at −20 °C on a MAR diffractometer with a 300 mm image plate detector using graphite-monochromatized Mo Kα radiation (λ = 0.710 73 Å). Data collection was made with 2° oscillation step of φ, 10-min exposure time, and scanner distance at 120 mm. A total of 100 images were collected. The images were interpreted and intensities integrated using the program DENZO.[18a] The structure was solved by direct methods employing the program SHELXS-97[18b] on a PC. Rhenium and most non-hydrogen atoms were found after successful refinement by full-matrix least-squares using the program SHELXL-97.[18b] There was one formula unit. One anion was located with disorder in the mode of shift. The noncoordination site of the ligand was also disordered in the mode of shift, by sharing one carbon atom. Restrains were applied to the disordered fragments, assuming the corresponding bond lengths were similar. One crystallographic asymmetric unit consisted of one formula unit, including one $CF_3SO_3^-$ anion. In the final stage of least-squares refinement, disordered atoms (except the sulfur atom of the anion) were refined isotropically; other non-hydrogen atoms were refined anisotropically. Hydrogen atoms (except that on the atom N(4)) were generated by the program SHELXL-97. The positions of hydrogen atoms were calculated on the basis of the riding mode with thermal parameters equal to 1.2 times that of the associated carbon atoms and participated in the calculation of final R-indices.

Equipment for characterization and electrochemical and photophysical measurements has been reported previously.[17d] Luminescence quantum yields were measured by the optically dilute method[19a] using an aerated aqueous solution of [Ru(bpy)$_3$]Cl$_2$

(18) (a) DENZO: Otwinowski, Z.; Minor, W. *Methods in Enzymology*; Academic Press: San Diego, CA, 1997; Vol, 276, p 307. (b) SHELXS-97 and SHELXL-97: Sheldrick, G. M. *Programs for Crystal Structure Analysis (Release 97-2)*; University of Göttingen: Göttingen, Germany, 1997.

(19) (a) Demas, J. N.; Crosby, G. A. *J. Phys. Chem.* **1971**, *75*, 991−1024. (b) Nakamura, K. *Bull. Chem. Soc. Jpn.* **1982**, *55*, 2697−2705.

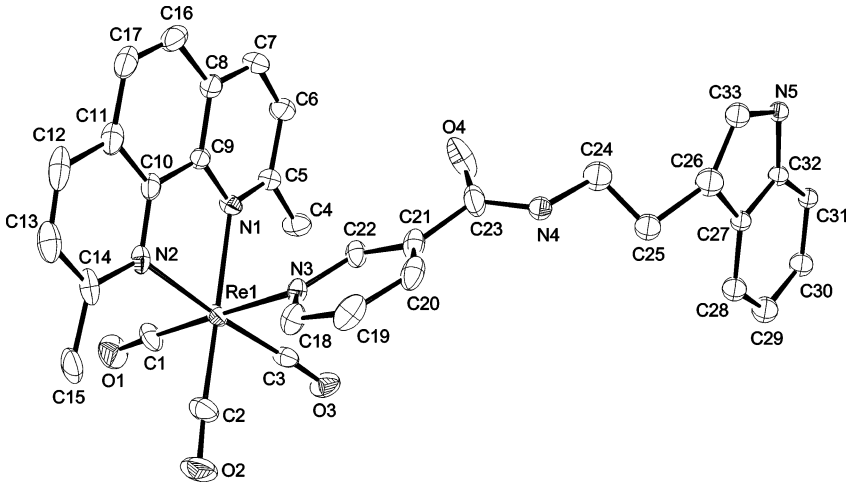

Figure 1. Perspective drawing of the cation of complex **3a**. Thermal ellipsoids are set at 20% probability.

($\Phi = 0.028$)[19b] as the standard solution. In transient absorption experiments, the monitoring light beam was generated from a 250 W quartz−tungsten−halogen lamp placed perpendicular to the excitation beam. The output of the quartz−tungsten−halogen lamp was wavelength selected by passing through two monochromators. The transient absorption signals were detected by a Hamamatsu R928 photomultiplier tube, amplified by a Tektronix AM502 differential amplifier (<1 MHz), and then digitized on a Tektronix TDS 620A digital oscilloscope that was interfaced to an IBM-compatible computer for data acquisition and analysis. The transient absorption difference spectra were generated using the point-to-point method.

For the determination of self-quenching rate constants (k_{sq}) of the complexes in CH_3CN, the following equation was adopted:

$$\frac{1}{\tau} = \frac{1}{\tau_{i.d.}} + k_{sq}[Re] \quad (1)$$

Here τ is the emission lifetime of the complex at concentration [Re] and $\tau_{i.d.}$ is the emission lifetime of the complex at infinite dilution. The slope and *y*-intercept of the linear fit of a plot of τ^{-1} vs [Re] gave k_{sq} and $\tau_{i.d.}{}^{-1}$, respectively.

Stern−Volmer quenching was studied by lifetime emission measurements of the complex in CH_3CN in the presence of a quencher at a concentration [*Q*]. The data were treated by a Stern−Volmer fit as follows:

$$\frac{\tau_o}{\tau} = 1 + k_q\tau_o[Q] \quad (2)$$

Here τ_o and τ are the excited-state lifetimes of the complex in the absence and presence of quencher, respectively, and k_q is the bimolecular quenching rate constant.

Emission Titrations with BSA. The rhenium(I) diimine complex (0.12 μmol) in 50 μL of 50 mM potassium phosphate buffer at pH 7.4/MeOH solution (1:1 v/v) was added to a series of phosphate buffer solutions (450 μL) containing BSA at various concentrations (1×10^{-3}−1×10^{-4} M). The solutions were gently stirred in the dark at room temperature for 12 h. The emission spectra of the solutions were then measured and compared to that of the control solutions in which BSA was absent.

For the determination of binding constants (K_a) of the complexes with BSA, the Scatchard equation was used:

$$\frac{\upsilon}{[Re]_{free}} = nK_a - \upsilon K_a \quad (3)$$

Here $\upsilon = [Re]_{bound}/[BSA]$, $[Re]_{free}$ and $[Re]_{bound}$ are the concentrations of the free and bound forms of the complex, respectively, [BSA] = concentration of BSA, and *n* is the binding stoichiometry. $[Re]_{bound}$ was calculated using the following equation:

$$[Re]_{bound} = [Re]_{total}\frac{[1 - (I/I_o)]}{1 - P} \quad (4)$$

Here $[Re]_{total}$ = total concentration of the complex, *I* and I_o are the emission intensity of the complex in the presence and absence of BSA, respectively, and *P* is $(I/I_o)_{max}$, which can be obtained as 1/(*y*-intercept) from the linear plot of I_o/I vs $[BSA]^{-1}$.

Tryptophanase Inhibition Assays. The rhenium(I) diimine complex or indole (0.10 μmol) in 100 μL of phosphate buffer/MeOH solution (2:1 v/v) was added to a mixture of pyridoxal 5-phosphate (0.125 μmol), lactate dehydrogenase (8.225 U), NADH (0.70 μmol), and L-serine at various concentrations in 1.57 mL of 0.15 M potassium phosphate buffer at pH 8.1 in an absorption cuvette. The temperature of the solution was thermostated at 37 °C for 15 min. The conversion of L-serine to pyruvate was initiated by addition of TPase (5 U in 830 μL of phosphate buffer) to the mixture. The concentration of L-serine in the cuvette varied from 100 to 800 mM. The percentage of inhibition of TPase was determined by comparing the decrease of absorbance of the solution at 340 nm to that of the control in which the rhenium(I) diimine indole complex or free indole was absent.

Results and Discussion

Synthesis. The luminescent rhenium(I) diimine complexes were prepared in moderate yields from the reaction of $[Re(N-N)(CO)_3(CH_3CN)](CF_3SO_3)$ with the ligands py-3-$CONHC_2H_4$-indole, py-3-$CONHC_5H_{10}CONHC_2H_4$-indole, or py-3-CONH-Et in refluxing THF. All the new rhenium(I) diimine complexes were characterized by ^{1}H NMR, positive-ion ESI-MS, and IR and gave satisfactory elemental analyses. The X-ray crystal structure of complex **3a** has been investigated.

Crystal Structure Determination. The perspective view of the cation of complex **3a** is depicted in Figure 1. The crystal determination data and selected bond lengths and angles are listed in Tables 1 and 2, respectively. The rhenium(I) center of complex **3a** adopted a distorted octahedral coordination geometry and the carbonyls were ar-

Table 1. Crystal Data and Summary of Data Collection and Refinement for Complex **3a**

formula	$C_{34}H_{27}F_3N_5O_7ReS$
fw	892.87
cryst size (mm^3)	0.4 × 0.2 × 0.1
T (K)	253
cryst syst	orthorhombic
space group	Pbca
a (Å)	19.487(4)
b (Å)	13.489(3)
c (Å)	25.289(5)
V ($Å^3$)	6647(2)
Z	8
ρ_{calcd} (g cm^{-3})	1.784
μ (mm^{-1})	3.793
F(000)	3520
θ range (deg)	2.00−25.54
index ranges	$-23 \le h \le 21$
	$-14 \le k \le 14$
	$-30 \le l \le 30$
no. of unique data/restraints/params	5763/68/424
R_{int}[a]	0.0433
GOF on F^2 [b]	1.028
R_1, wR_2 ($I > 2\sigma(I)$)[c]	0.0433, 0.1176
R_1, wR_2 (all data)	0.0597, 0.1229
largest diff peak/hole (e $Å^{-3}$)	1.221, −1.650

[a] $R_{int} = \Sigma|F_o^2 - F_o^2(\text{mean})|/\Sigma[F_o^2]$. [b] GOF $= \{\Sigma[w(F_o^2 - F_c^2)^2]/(n-p)\}^{1/2}$, where n is the number of reflections and p is the total number of parameters refined. The weighting scheme is $w = 1/[\sigma^2(F_o^2) + (aP)^2 + (bP)]$, where P is $[2F_c^2 + \max(F_o^2,0)]/3$, $a = 0.0723$, and $b = 0.0000$. [c] $R_1 = \Sigma||F_o| - |F_c||/\Sigma|F_o|$; $wR_2 = \{\Sigma[w(F_o^2 - F_c^2)^2]/\Sigma[w(F_o^2)^2]\}^{1/2}$.

Table 2. Selected Bond Lengths (Å) and Bond Angles (deg) for Complex **3a**

Re(1)−N(1)	2.207(5)	Re(1)−N(2)	2.207(5)
Re(1)−N(3)	2.220(5)	Re(1)−C(1)	1.914(8)
Re(1)−C(2)	1.897(8)	Re(1)−C(3)	1.909(8)
C(1)−Re(1)−C(2)	86.7(4)	C(1)−Re(1)−C(3)	88.6(3)
C(1)−Re(1)−N(1)	97.4(3)	C(1)−Re(1)−N(2)	95.4(3)
C(1)−Re(1)−N(3)	179.1(3)	C(2)−Re(1)−C(3)	83.1(3)
C(2)−Re(1)−N(1)	174.3(3)	C(2)−Re(1)−N(2)	99.5(3)
C(2)−Re(1)−N(3)	92.7(3)	C(3)−Re(1)−N(1)	101.0(2)
C(3)−Re(1)−N(2)	175.3(2)	C(3)−Re(1)−N(3)	90.6(3)
N(1)−Re(1)−N(2)	76.2(2)	N(1)−Re(1)−N(3)	83.22(19)
N(2)−Re(1)−N(3)	85.40(18)		

ranged in a *facial* orientation. The Re−N and Re−C bond lengths varied from 2.207(5) to 2.220(5) Å and from 1.897(8) to 1.914(8) Å, respectively. These bond lengths were comparable to those of related systems including $[Re(bpy)(CO)_3(py)][Co(CO)_4]$ (Re−N, 2.156(13)−2.213(14) Å; Re−C, 1.88(2)−1.98(2) Å),[8c] [Re(3,3′-trimethylene-2,2′-bpy)$(CO)_3$(Br)] (Re−N, 2.20(1)−2.21(1) Å; Re−C, 1.91(1)−1.92(2) Å),[11a] $[Re(bpy)(CO)_3(O_2C\text{-}pz)]$ (Re−N, 2.162(8)−2.164(8) Å; Re−C, 1.883(11)−1.909(11) Å),[11b] $[Re(N{-}N)(CO)_3(py)]^+$ (N−N = dppz, dppn) (Re−N, 2.16(1)−2.206(6) Å; Re−C, 1.85(2)−1.937(8) Å),[16] $[Re(Me_2\text{-phen})(CO)_3(py\text{-}3\text{-}mal)]^+$ (Re−N, 2.199(7)−2.219(6) Å; Re−C, 1.90(1)−1.918(10) Å),[17a] and $[Re(Me_4\text{-phen})(CO)_3(py\text{-}Ph)]^+$ (Re−N, 2.171(4)−2.220(4) Å; Re−C, 1.919(6)−1.937(6) Å)[17d] and the previously reported rhenium(I) diimine indole complexes **1a**,**b** (Re−N, 2.167(6)−2.253(3) Å; Re−C, 1.888(7)−1.930(6) Å).[17c] The bite angle of the Me_2-phen ligand (N1−Re−N2 = 76.2(2)°) was also comparable to those observed in other related systems (74.2(3)−75.6(14)°).[8c,11a,b,16,17a,c,d] The indole moiety of complex **3a** exhibited a dihedral angle of ca. 7.29° with the Me_2-phen ligand of the same molecule. Interestingly, unlike complexes **1a**,**b**, complex **3a** did not display any stacking interactions between the diimine ligand and indole unit of two neighboring molecules.

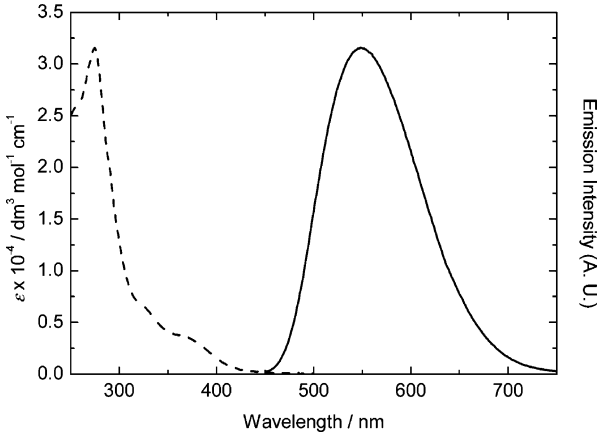

Figure 2. Electronic absorption (---) and emission (−) spectra of complex **2a** in CH_3CN at 298 K.

Electrochemical Properties. The electrochemical properties of the complexes have been studied by cyclic voltammetry. The electrochemical data are summarized in Table 3. All the complexes displayed quasi-reversible/irreversible rhenium(II/I) oxidation at ca. +1.7 to +1.8 V vs SCE.[7,8c,10,11,12a,13a,14,17c,d] Additionally, quasi-reversible/irreversible couples were also observed at ca. +1.1 to +1.4 V for the indole-containing complexes. These features are assigned to the oxidation of the indole moieties of the pyridine ligands because similar waves at comparable potentials were observed for the uncoordinated ligands (ca. +1.1 and +1.3 V). With reference to previous electrochemical studies of related rhenium(I) diimine systems,[7,8c,10,11,12a,13a,14,17c,d] we attribute the first reduction waves of all the complexes to the reduction of the diimine ligands. This is in agreement with the fact that the electron-donating methyl substituents rendered the first reduction of the Me_4-phen (ca. −1.4 V) and Me_2-phen (ca. −1.2 V) complexes to occur at more negative potentials than those of the phen (ca. −1.1 V) and Ph_2-phen (ca. −1.1 V) complexes. In addition, all the complexes showed quasi-reversible/irreversible waves at more negative potentials. Although the exact origin of these reduction waves is unknown at this stage, those at ca. −1.6 V could be associated with the rhenium(I/0) couple.[11,14b]

Electronic Absorption and Emission Properties. The electronic absorption spectral data of the rhenium(I) diimine complexes are summarized in Table 4. The electronic absorption spectrum of complex **2a** in CH_3CN at 298 K is shown in Figure 2. The electronic absorption spectra of these complexes revealed strong absorption bands at ca. 247−328 nm and less intense absorption shoulders at ca. 324−384 nm, which are assigned to ligand-centered (^{1}IL) ($\pi \rightarrow \pi^*$) (diimine and pyridine ligands) and spin-allowed metal-to-ligand charge-transfer (^{1}MLCT) ($d\pi(Re) \rightarrow \pi^*$(diimine)) transitions, respectively.[5−17] However, it is likely that the absorption shoulders of the Ph_2-phen complexes **4a**−**c** at ca.

Table 3. Electrochemical Data of the Rhenium(I) Diimine Complexes[a]

complex	oxidn $E_{1/2}$ or E_a/V	redn $E_{1/2}$ or E_c/V
1a	+1.10,[b] +1.29,[c] +1.71[c]	−1.43,[b] −1.63,[c] −1.80,[c] −1.92,[c] −2.25[c]
1b	+1.09,[b] +1.68[c]	−1.41,[c] −1.64,[c] −1.80,[c] −1.96,[c] −2.28[c]
1c	+1.69[c]	−1.42,[c] −1.63,[c] −1.78,[c] −1.93,[c] −2.25[c]
2a	+1.10,[b] +1.37,[c] +1.75[c]	−1.12,[c] −1.20,[c] −1.61,[c] −1.75,[c] −2.28[b]
2b	+1.15,[b] +1.75[c]	−1.14,[c] −1.24,[c] −1.55,[c] −1.78,[c] −2.26[c]
2c	+1.85[b]	−1.16,[b] −1.25,[b] −1.58,[c] −1.74,[c] −2.24[b]
3a	+1.10,[b] +1.34,[c] +1.81[c]	−1.20,[b] −1.32, −1.48,[b] −1.63,[b] −1.90,[c] −2.25,[b] −2.32[c]
3b	+1.10,[b] + 1.79[c]	−1.20,[b] −1.28,[c] −1.46,[c] −1.62,[c] −1.90,[c] −2.24,[b] −2.39[c]
3c	+1.82[b]	−1.20,[b] −1.32,[b] −1.46,[c] −1.64,[b] −1.85, −2.22,[b] −2.37[b]
4a	+1.10,[b] +1.79[b]	−1.12,[c] −1.23,[c] −1.43,[c] −1.61,[c] −2.09,[c] −2.20[c]
4b	+1.05,[b] +1.82[b]	−1.12, −1.21,[b] −1.34,[b] −1.45, −1.63, −2.10,[b] −2.26
4c	+1.83[b]	−1.13,[c] −1.23,[b] −1.44,[c] −1.61,[c] −2.09,[c] −2.20[b]

[a] In CH_3CN (0.1 mol dm^{-3} $^nBu_4NPF_6$) at 298 K, glassy carbon electrode, sweep rate 100 mV s^{-1}; all potentials versus SCE. [b] Irreversible waves. [c] Quasi-reversible waves.

Table 4. Electronic Absorption Spectral Data of the Rhenium(I) Diimine Complexes at 298 K

complex	medium	λ_{abs}/nm (ϵ/dm^3 mol^{-1} cm^{-1})
1a	CH_3CN	250 sh (33 540), 280 (39 525), 290 sh (32 110), 308 sh (16 515), 370 sh (3375)
	MeOH	250 sh (29 890), 280 (34 995), 290 sh (28 465), 310 sh (13 920), 370 sh (3165)
1b	CH_3CN	247 sh (31 295), 281 (37 640), 292 sh (27 870), 323 sh (11 245), 368 sh (3370)
	MeOH	249 sh (32 485), 281 (38 300), 291 sh (29 865), 328 sh (10 180), 371 sh (3370)
1c	CH_3CN	249 sh (32 570), 281 (34 870), 316 sh (14 130), 371 sh (3540)
	MeOH	247 sh (35 595), 281 (38 230), 310 sh (11 215), 369 sh (4025)
2a	CH_3CN	254 sh (25 705), 274 (31 475), 290 sh (20 090), 330 sh (6010), 368 sh (3350)
	MeOH	254 sh (27 795), 276 (33 220), 290 sh (21 755), 330 sh (6765), 370 sh (4005)
2b	CH_3CN	256 sh (27 895), 275 (35 150), 289 sh (23 115), 325 sh (6900), 368 sh (3775)
	MeOH	254 sh (24 710), 275 (30 475), 291 sh (19 335), 322 sh (6315), 367 sh (3475)
2c	CH_3CN	252 sh (22 080), 276 (26 130), 324 sh (6295), 368 sh (3495)
	MeOH	252 sh (26 185), 276 (29 965), 324 sh (7350), 368 (4185)
3a	CH_3CN	282 (24 005), 310 sh (11 120), 383 sh (1715)
	MeOH	283 (26 975), 312 sh (12 205), 383 sh (2220)
3b	CH_3CN	282 (24 990), 312 sh (10 705), 380 sh (1945)
	MeOH	282 (26 445), 310 sh (12 255), 383 sh (2175)
3c	CH_3CN	283 (20 730), 308 sh (12 140), 377 sh (2045)
	MeOH	284 (22 770), 312 sh (12 500), 377 sh (2480)
4a	CH_3CN	260 sh (27 150), 292 (41 025), 334 sh (14 440), 384 sh (6440)
	MeOH	258 (24 785), 292 (38 545), 334 sh (13 905), 384 sh (6430)
4b	CH_3CN	257 sh (29 400), 290 (45 605), 334 sh (16 230), 384 sh (7110)
	MeOH	259 (27 835), 291 (42 315), 334 sh (15 280), 384 sh (6980)
4c	CH_3CN	260 sh (27 310), 292 (42 650), 334 sh (16 065), 384 sh (7325)
	MeOH	260 sh (26 970), 292 (41 720), 334 sh (16 385), 384 sh (7640)

334 nm possessed substantial ^{1}IL character in view of the phenyl substituents of the diimine ligand. Accordingly, the ^{1}MLCT ($d\pi(Re) \rightarrow \pi^*(Ph_2\text{-phen})$) transitions of these Ph_2-phen complexes occurred at further lower energy at ca. 384 nm.

Upon visible-light excitation, all the complexes displayed green to orange-yellow luminescence under ambient conditions and in alcohol glass. The photophysical data are tabulated in Table 5. The emission spectrum of complex **2a** in CH_3CN at 298 K is shown in Figure 2. In fluid solutions at 298 K, the indole-containing complexes displayed emission at energy that was similar to that of their indole-free counterparts (Table 5). The solution emission of these indole-containing complexes is generally assigned to an ^{3}MLCT ($d\pi(Re) \rightarrow \pi^*$(diimine)) excited state.[5,6,7a−c,e,8b,c,9,10,11b,12−14,17] However, long emission lifetimes of the Me_4-phen complexes **1a**−**c** in solutions at room temperature (Table 5) suggest that the excited state of these complexes exhibited substantial ^{3}IL ($\pi \rightarrow \pi^*$) (Me_4-phen) character. Similar assignments have been reported for related complexes.[6,14b,17] For example, Rillema and co-workers reported that emission lifetime of the complex $[Re(Me_4\text{-phen})(CO)_3(py)]^+$ is only slightly affected by solvent environment and its temperature dependence is different to those of related complexes.[6a] These observations were attributed to the contribution of an ^{3}IL state to the luminescence of the complex at room temperature. In another study, calculations of the complexes $[M(CO)_4(N-N)]$ (M = Cr or W; N−N = phen or Me_4-phen) showed that the LUMO's of the phen and Me_4-phen complexes are of b_1 and a_2 symmetry, respectively.[20] The exceptionally long emission lifetime of $[W(CO)_4(Me_4\text{-phen})]$ as compared to $[W(CO)_4(phen)]$ was ascribed to the different contributions of individual orbital excitations to the excited states involved.

In this work, when the indole-containing complexes were excited in the ultraviolet region (λ_{ex} = 250 nm), they exhibited an additional emission band at ca. 365 nm that originated from the indole moiety. The emission intensity was ca. 150−1300 times lower than that of free indole in CH_3CN and MeOH ($A_{250\ nm}$ = 0.1). The generally weak indole emission of the complexes can be accounted for by the fact that the rhenium(I)−diimine moieties of these complexes absorbed very strongly at the excitation wavelength (for example $\epsilon_{250\ nm}$ = 33 540 dm^3 mol^{-1} cm^{-1} for complex **1a** in CH_3CN at 298 K). Another possible reason

(20) Farrell, I. R.; Hartl, F.; Záliš, S.; Mahabiersing, T.; Vlček, A., Jr. *J. Chem. Soc., Dalton Trans.* **2000**, 4323−4331.

Table 5. Photophysical Data of the Rhenium(I) Diimine Complexes

complex	medium (T/K)	λ_{em}/nm[a]	τ/μs[a]	Φ[b]
1a	CH_3CN (298)	518	8.21	0.0085
	MeOH (298)	516	8.60	0.0083
	buffer[c] (298)	516	8.14	0.0057
	glass[d] (77)	464, 497, 530 sh	86.38 (52%), 19.77 (48%)	
1b	CH_3CN (298)	514	6.33	0.0091
	MeOH (298)	520	6.19	0.0035
	buffer[c] (298)	514	6.11	0.0053
	glass[d] (77)	465, 497, 533, 540 sh	95.17 (49%), 21.43 (51%)	
1c	CH_3CN (298)	515	14.12	0.54
	MeOH (298)	516	14.25	0.39
	buffer[c] (298)	515	12.83	0.25
	glass[d] (77)	464, 497, 534 sh, 577 sh	117.65 (44%), 28.98 (56%)	
2a	CH_3CN (298)	548	1.91	0.021
	MeOH (298)	548	1.36	0.019
	buffer[c] (298)	550	1.06	0.014
	glass[d] (77)	476 sh, 494	10.11	
2b	CH_3CN (298)	545	1.87	0.020
	MeOH (298)	547	1.31	0.016
	buffer[c] (298)	548	1.09	0.0093
	glass[d] (77)	462 sh, 497	10.23	
2c	CH_3CN (298)	548	2.11	0.33
	MeOH (298)	546	1.56	0.23
	buffer[c] (298)	548	1.16	0.17
	glass[d] (77)	476 sh, 494	11.21	
3a	CH_3CN (298)	530	1.79	0.0076
	MeOH (298)	532	1.66	0.0059
	buffer[c] (298)	532	1.47	0.0049
	glass[d] (77)	475 sh, 496	15.31	
3b	CH_3CN (298)	534	1.62	0.038
	MeOH (298)	537	1.72	0.018
	buffer[c] (298)	536	1.55	0.0089
	glass[d] (77)	470 sh, 497	15.67	
3c	CH_3CN (298)	536	2.30	0.30
	MeOH (298)	531	2.57	0.30
	buffer[c] (298)	533	2.10	0.24
	glass[d] (77)	475 sh, 497	15.69	
4a	CH_3CN (298)	558	4.38	0.029
	MeOH (298)	556	3.96	0.021
	buffer[c] (298)	561	2.99	0.015
	glass[d] (77)	508, 534 sh	22.78	
4b	CH_3CN (298)	554	3.82	0.037
	MeOH (298)	556	3.62	0.036
	buffer[c] (298)	561	3.05	0.016
	glass[d] (77)	508, 534 sh	22.99	
4c	CH_3CN (298)	560	6.06	0.34
	MeOH (298)	556	5.04	0.27
	buffer[c] (298)	562	3.36	0.18
	glass[d] (77)	508, 534 sh	23.68	

[a] $\lambda_{ex} = 355$ nm, [Re] = 50 μM. [b] $\lambda_{ex} = 355$ nm, $A_{355\ nm} = 0.1$. [c] 50 mM potassium phosphate at pH 7.4 containing 20% MeOH (MeOH was used for solubility reasons). [d] EtOH/MeOH (4:1 v/v).

is that the indole moiety emitted at a wavelength (ca. 365 nm) where the rhenium(I) diimine units absorbed quite strongly, resulting in resonance energy transfer from the indole to the luminophore.[21]

Upon cooling of samples to low temperature, all the complexes displayed a blue-shift in the emission maxima. These rigidochromic shifts are in line with the charge-transfer emissive states of the complexes.[5,9a,10a,12,17c,d] In alcohol glass, most of the complexes exhibited an emission lifetime of ca. 10−29 μs, and the emissive state is likely to be ^{3}MLCT in nature.[5,9a,10a,12,17c,d] However, biexponential decays were observed for Me_4-phen complexes **1a**−**c**, and the longer-lived (ca. 120−86 μs) component is assigned to an ^{3}IL (Me_4-phen) excited state.[17c,d] The shorter-lived component (ca. 30−20 μs) is of the same order of magnitude compared to other complexes in this work and is assigned to an ^{3}MLCT emissive state.

Table 6. Self-Quenching Rate Constants and Emission Lifetimes (at Infinite Dilution) of the Rhenium(I) Diimine Indole Complexes in CH_3CN at 298 K

complex	k_{sq}/dm^3 mol^{-1} s^{-1}	$\tau_{i.d.}$/μs
1a	9.6×10^8	13.86
1b	1.5×10^9	13.72
2a	9.5×10^8	2.10
2b	1.3×10^9	2.10
3a	1.7×10^9	2.14
3b	2.2×10^9	2.02
4a	1.0×10^9	6.03
4b	1.5×10^9	6.02

It is interesting to note that the indole-containing complexes exhibited much lower luminescence quantum yields and shorter emission lifetimes than those of their indole-free counterparts (Table 5). Also, unlike their indole-free counterparts, these complexes displayed concentration-dependent emission lifetimes, suggesting a self-quenching process in which the emission of the rhenium(I)−diimine moiety was quenched by the indole unit. With reference to eq 1, the self-quenching rate constants (k_{sq}) and lifetimes at infinite dilution ($\tau_{i.d.}$) of the indole-containing complexes in CH_3CN have been determined from plots of τ^{-1} vs [Re] (Table 6). These emission lifetimes were comparable to those of the indole-free complexes **1c**−**4c** (Table 5), indicative of the importance of intermolecular interactions in the self-quenching of the complexes. Since the triplet-state energy of indole (ca. 24 800 cm^{-1})[22,23] is much higher than the emission energy of the indole-containing complexes and there was no spectral overlap between the emission spectra of the indole-free complexes and the absorption spectrum of indole, it is unlikely that the self-quenching of the indole-containing complexes occurred via an energy-transfer mechanism. From the potentials of the diimine-based reduction of $[Re(N-N)(CO)_3(py\text{-}3\text{-}CONH\text{-}Et)]^+$ (between ca. −1.1 and −1.4 V vs SCE) and the low-temperature emission energy of $[Re(N-N)(CO)_3(py\text{-}3\text{-}CONH\text{-}Et)]^+$ (E^{00} = 2.44−2.67 eV), the excited-state reduction potentials, $E°[Re^{+*/0}]$, were estimated to be ca. +1.25 to +1.49 V vs SCE. On the basis of these potentials and the redox potential of indole ($E°[indole^{+/0}] <$ +1.06 V vs SCE, which was obtained from the cyclic voltammetric studies of the pyridine−indole ligands), reductive quenching of the excited complexes by indole is favored by >0.2−0.4 eV (Table 7). It is likely that the mechanism of the emission quenching of the indole-containing complexes is electron transfer in nature.

To gain more insight into the quenching mechanism, Stern−Volmer studies on the indole-free complexes using indole as a quencher have been carried out. The Stern−

(21) Wu. P.; Brand, L. *Anal. Biochem.* **1994**, *218*, 1−13.

(22) Klein, R.; Tatischeff, I.; Bazin, M.; Santua, R. *J. Phys. Chem.* **1981**, *85*, 670−677.

(23) Kasama, K.; Takematsu, A.; Aral, S. *J. Phys. Chem.* **1982**, *86*, 2420−2427.

Table 7. Standard Free Energy Change and Bimolecular Quenching Rate Constants for the Quenching of Complexes **1c**−**4c** by Indole in CH_3CN at 298 K

complex	ΔG/eV[a]	k_q/dm^3 mol^{-1} s^{-1}	k_q/dm^3 mol^{-1} s^{-1} [b]
1c	−0.19	5.6×10^8	5.8×10^8
2c	−0.39	3.1×10^9	3.7×10^9
3c	−0.35	4.1×10^9	5.2×10^9
4c	−0.25	3.0×10^9	3.5×10^9

[a] Estimated from glass emission and electrochemical data; see text for details. [b] $(1/k_{q'}) = (1/k_q) - (1/k_d)$, where k_d is the diffusion-limited rate constant (2.0×10^{10} dm^3 mol^{-1} s^{-1}).

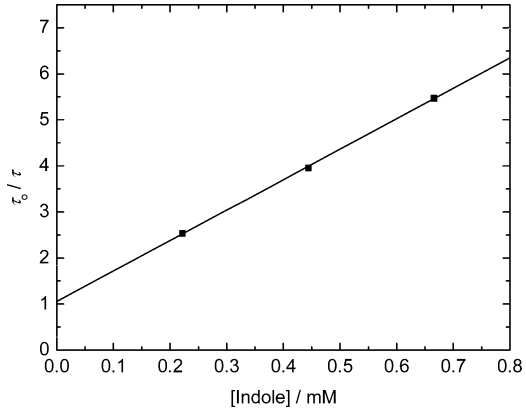

Figure 3. Stern−Volmer plot for the emission quenching of complex **2c** by indole.

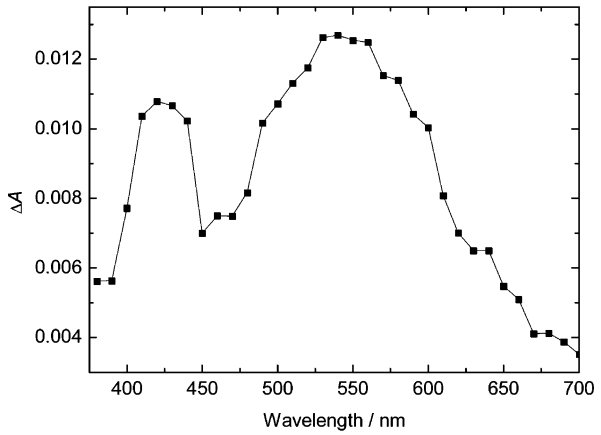

Figure 4. Transient absorption difference spectrum of a degassed acetonitrile solution of complex **3c** (5.5 mM) and indole (55 mM) at 298 K recorded 6 μs after laser flash.

Volmer plot for complex **2c** is shown in Figure 3. The bimolecular quenching rate constants were in the order of 10^8−10^9 dm^3 mol^{-1} s^{-1} (Table 7). These values were comparable to the self-quenching rate constants of the indole-containing complexes (Table 6), suggesting that intermolecular electron transfer played a key role in the self-quenching of the indole-containing complexes. In an attempt to obtain more direct spectroscopic information on the mechanism of the photoreactions between the indole-free complexes **1c**−**4c** and indole, nanosecond transient absorption experiments have been performed. For example, the transient absorption difference spectrum of an acetonitrile solution of complex **3c** and indole at 298 K recorded 6 μs after laser flash is shown in Figure 4. The spectrum displayed an absorption band at ca. 420 nm and a broader one of higher

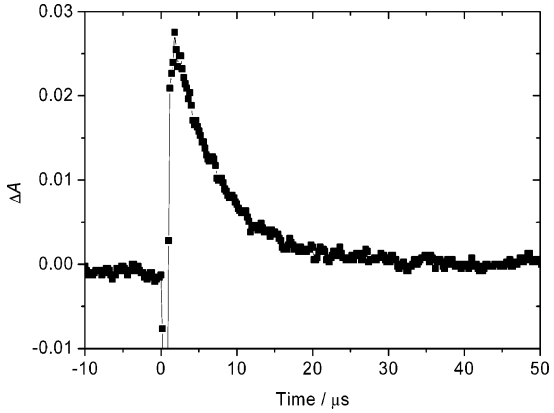

Figure 5. Decay trace of the transient absorption band at 550 nm of a degassed acetonitrile solution of complex **3c** (5.5 mM) and indole (55 mM) at 298 K.

intensity at ca. 550 nm. The decay trace at 550 nm is shown in Figure 5. It is unlikely that these bands are associated with the diimine-localized anion of the rhenium(I) diimine complex, $[Re^I(CO)_3(Me_2\text{-phen}^{\cdot -})(py\text{-}3\text{-}CONH\text{-}Et)]^0$, because the absorption band of the diimine anion radical is expected to occur at ca. 350−400 nm.[7b,8c,15] With reference to the pulse radiolysis and transient absorption studies of a series of indole derivatives,[23−25] we believe that these bands at ca. 420 and 550 nm were due to the absorption of the indolyl radical. Thus, the transient absorption spectrum is a proof that the emission quenching of the complexes by indole is electron transfer in nature. However, the decay traces of these bands did not return completely to the baselines, suggesting that there may be some photochemical reactions in addition to back-electron-transfer.

Emission Titrations with BSA. Albumins are responsible for important physiological functions in living organisms. The principal role of these proteins is to assist the metabolism, transport, and distribution of exogenous and endogenous substances.[26] Additionally, it is well-known that albumins can bind indole, tryptophan, and their derivatives.[26,27] In view of this, the interactions of the rhenium(I) diimine indole complexes with one of these proteins, BSA, have been studied by emission titrations. Our results showed that the emission intensity of the indole-containing complexes was enhanced in the presence of BSA. As an example, results of the emission titration of complex **3a** with BSA are illustrated in Figure 6. At [BSA] = 1 mM, the indole-containing complexes revealed up to a 17-fold increase in emission intensity and a 2-fold increase in emission lifetimes (Table 8). These observations are ascribed to the specific binding of the indole moiety of the complexes to the protein because no similar changes were observed for the indole-free complexes. Since the emission quantum yields of the indole-free complexes were already very high (Table 5), one may argue that even if these complexes bound to BSA, their

(24) Jovanovic, S. V.; Steenken, S. *J. Phys. Chem.* **1992**, *96*, 6674−6679.
(25) Crespo, A.; Turjanski, A. G.; Estrin, D. A. *Chem. Phys. Lett.* **2002**, *365*, 15−21.
(26) Carter, D. C.; Ho, J. X. *Adv. Protein Chem.* **1994**, *45*, 153−203.
(27) McMenamy, R. H.; Oncley, J. L. *J. Biol. Chem.* **1958**, *233*, 1436−1447.

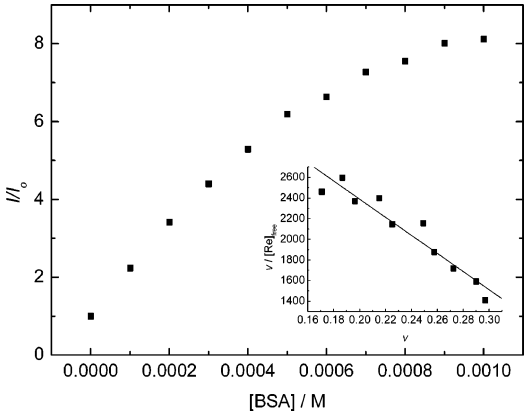

Figure 6. Results of emission titration of complex **3a** with BSA. I_o and I are the emission intensity of the complex in the absence and presence of BSA, respectively. The inset shows the Scatchard plot.

Table 8. Results of Titrations of the Rhenium(I) Diimine Indole Complexes with BSA in 50 mM Potassium Phosphate Buffer at pH 7.4 at 298 K

complex	I/I_o[a]	τ/τ_o[b]	K_a[c]	n
1a	2.4	1.7	1.0×10^4	0.6
1b	17.1	2.0	1.7×10^4	0.7
2a	2.1	1.3	0.9×10^4	0.5
2b	3.2	1.3	1.1×10^4	0.8
3a	8.1	1.6	0.9×10^4	0.5
3b	5.0	1.3	1.1×10^4	0.7
4a	1.0	1.1	*d*	*d*
4b	1.1	1.1	*d*	*d*

[a] I_o and I are the emission intensity of the rhenium(I) diimine indole complexes in the presence of 0 and 1 mM BSA, respectively. [b] τ_o and τ are the emission lifetimes of the rhenium(I) diimine indole complex in the presence of 0 and 1 mM BSA, respectively. [c] The uncertainties of K_a are estimated to be ±10%. [d] K_a and n could not be determined with accuracy due to the small changes in emission intensity.

emission intensity would not be significantly enhanced. However, it is noteworthy that all the indole-free complexes did not show any increase in emission lifetimes, indicating of the lack of protein-binding properties for these complexes. Previous studies showed that tryptamine and its derivatives bind to a specific hydrophobic site of BSA.[26,28] We believe that the increase in the emission intensity and lifetimes of the indole-containing complexes was closely related to the enhanced hydrophobicity and rigidity of their local surroundings upon binding to the protein. The reason is that common rhenium(I) diimine complexes showed higher emission quantum yields and longer lifetimes in more nonpolar solvents.[17a,b,d,e] Nevertheless, in the cases of the Ph_2-phen complexes **4a**,**b**, the emission properties did not show significant changes, which may be due to the relatively bulky Ph_2-phen ligand that disfavors the protein binding of these complexes.

The binding constants (K_a) for the complexes with BSA have been determined using eqs 3 and 4. A plot of $\upsilon/[Re]_{free}$ vs υ for complex **3a** is shown in the inset of Figure 6. The binding constants (K_a) and binding stoichiometry n are listed in Table 8. These values are comparable to those observed for the albumin binding of tryptamine ($K_a = 1.1 \times 10^4$ M^{-1}, $n = 1$),[28] indole-3-acetic acid ($K_a = 1.7 \times 10^4$ M^{-1}, $n = 1$)[28] and 5-hydroxyindole-3-acetic acid ($K_a = 2.0 \times 10^4$ M^{-1}, $n = 1$),[28] and a platinum(II) poly(ethylene glycol) complex ($K_a = 2.7 \times 10^4$ M^{-1}, $n = 1$).[29] In general, the binding constants of complexes **1b**−**3b** were slightly larger than those of complexes **1a**−**3a**,[30] revealing that longer spacer arms could minimize the steric hindrance between the rhenium(I)−diimine luminophore and the protein.

Table 9. Percentage Inhibition of TPase Activity by the Rhenium(I) Diimine Complexes and Indole at [L-Serine] = 800 mM and Michaelis Constants for the TPase Assays in 0.15 mM Potassium Phosphate Buffer of pH 8.0 at 310 K

complex	inhibition/%	K_m/mM
1a	61	143
1b	74	172
1c	3	166
2a	43	154
2b	72	179
2c	7	154
3a	64	161
3b	74	167
3c	8	157
4a	55	158
4b	77	176
4c	6	154
indole	53	149

Tryptophanase Inhibition Assays. The enzyme tryptophanase (TPase) catalyzes a variety of α,β-elimination and β-replacement reactions of amino acid substrates in the presence of the cofactor pyridoxal 5-phosphate.[31] For example, it converts common amino acid substrates, such as L-serine, L-tryptophan, and L-cysteine, to pyruvate and ammonium. Interestingly, it has been shown that indole inhibits the activity of this enzyme.[31] The inhibition of enzymatic activity by small molecules is important as it is a major mechanism to control biological systems. To study the possible inhibition of TPase by the rhenium(I) diimine indole complexes, a standard assay that is on the basis of the conversion of L-serine to pyruvate by the enzyme has been carried out.[31] The formation of pyruvate can be detected by coupling to the lactate dehydrogenase/NADH system. The reaction was monitored by measuring the decrease of the absorbance of the solution at 340 nm due to the consumption of NADH. Under our experimental conditions, at [L-serine] = 800 mM, free indole inhibited 53% of the enzyme activity, while the indole-containing complexes and their indole-free counterparts caused ca. 43−77 and 3−8% inhibition, respectively (Table 9). These results revealed that TPase can interact with these rhenium(I) diimine indole complexes instead of their indole-free counterparts. It appears that the inhibition originated from the binding of the indole moiety of the complexes to the enzyme. It is interesting to note that complexes **1b**−**4b** caused a higher extent of inhibition to the TPase-catalyzed reaction compared to complexes **1a**−**4a**, suggestive of the importance of the linker on alleviating the steric hindrance between the rhenium(I) diimine indole

(28) Okabe, N.; Adachi, K. *Chem. Pharm. Bull.* **1992**, *40*, 499−500.

(29) Che, C. M.; Zhang, J. L.; Lin, L. R. *Chem. Commun.* **2002**, 2556−2557.

(30) The uncertainties of K_a are estimated to be ±10%. Taking the experimental errors into consideration, the difference of K_a between complexes **1a** and **1b** is much more significant compared to those of complexes **2a** and **2b** and **3a** and **3b** (Table 8).

(31) Morino, Y.; Snell, E. E. *J. Bio. Chem.* **1967**, *242*, 2793−2799.

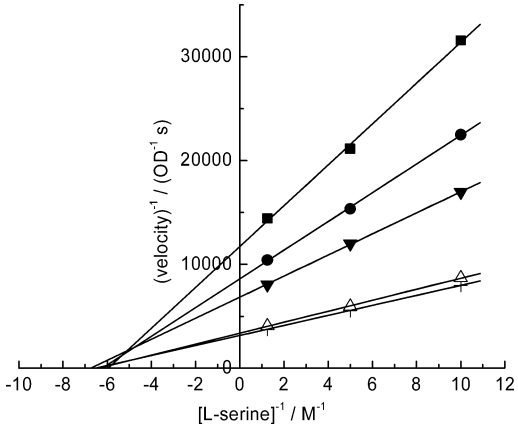

Figure 7. Plots of υ^{-1} vs [L-serine]$^{-1}$ for the TPase inhibition assays, in which complex **3a** (●), **3b** (■), or **3c** (△), indole (▼), or no inhibitor (+) was used.

complexes and the enzyme. On the basis of the results, the Michaelis constants (K_m) for the enzyme activity have been determined from plots of the linear transform of the Michaelis−Menten equation.[32] Plots of υ^{-1} vs [L-serine]$^{-1}$ for the TPase inhibition assays using complexes **3a**−**c**, indole, and no inhibitor are shown in Figure 7. From the *x*-intercepts of the linear fits, the K_m values for the complexes have been determined (Table 9). Since the *x*-intercepts of all the fits were very similar, the indole-containing complexes inhibited the TPase-catalyzed conversion of L-serine to pyruvate in a noncompetitive fashion. In other words, the inhibitors and substrate can bind simultaneously to TPase at two different sites, leading to the formation of a ternary intermediate. Note that unsubstituted indole also inhibits the activity of TPase in a similar way,[31] supporting the argument that the indole moiety of the current rhenium(I) complexes is responsible for the inhibition. The rhenium(I) diimine indole complexes showed similar K_m values, indicating that whereas the spacer arms could cause a higher degree of inhibition, they did not significantly affect the binding affinity of the substrate to the enzyme.

(32) Atkins, G. L.; Nimmo, I. A. *Biochem. J.* **1973**, *135*, 779−784.

Conclusion

In conclusion, we have synthesized a new series of luminescent rhenium(I) diimine indole complexes. The electrochemical, photophysical, and protein-binding properties of these new complexes have been studied. The results revealed that these complexes can be recognized by indole-binding proteins such as BSA and TPase. We anticipate that the protein-binding properties of related luminescent indole conjugates can provide an insight into protein−ligand interactions and that the complexes could be utilized as a new class of probes for indole-binding proteins.

Acknowledgment. We thank the Hong Kong Research Grants Council (Project No. CityU 101704) for financial support. K.H.-K.T. and W.-K.H. acknowledge the receipt of a Postgraduate Studentship and a Research Tuition Scholarship, both administered by the City University of Hong Kong.

Supporting Information Available: X-ray data (CIF) for complex **3a**. This material is available free of charge via the Internet at http://pubs.acs.org.

IC050531U